Comparative study of the structure and magnetic properties of Co-P and Fe-P amorphous alloys

A. García-Arribas, M. L. Fdez-Gubieda, and J. M. Barandiarán
Departamento de Electricidad y Electrónica, Universidad del País Vasco, Apartado Postal 644, 48080 Bilbao, Spain
(Received 12 February 1999; revised manuscript received 8 September 1999)

We present the structural parameters of a complete series of $Co_{1-x}P_x$ ($x=0.17-0.26$) amorphous alloys as obtained by the analysis of x-ray absorption fine structure measurements. To investigate their correlation with the magnetic properties, we have performed magnetization measurements in the same set of samples, obtaining the concentration dependence of the saturation magnetization, Curie temperature, and the behavior of the low-temperature magnetization. The results for the Co-P system are then compared with the ones of amorphous Fe-P, in order to clarify whether the different structural features found can be used to explain the different behavior of the magnetic properties that these systems exhibit. The evolution of the spontaneous magnetization with the metalloid content is the same for both systems. The Curie temperature decreases appreciably in Co-P, while remaining unchanged in Fe-P. The main result of the structural analysis shows that the bonding distances between metal atoms increases in the Co-P system, whereas they do not change in Fe-P. These magnetic and structural differences are correlated in basis of simple magnetic models.

I. INTRODUCTION

Due to their promising potential applications, the magnetic properties of amorphous magnetic materials of a wide variety of compositions, have been the subject of intensive research during the last decades. However, though the amount of compiled experimental data is huge,[1–3] there is still not a clear understanding of the fundamental aspects of the magnetism of such systems. As it is well assumed, the atomic structure plays a determinant role in the magnetic interactions, and its knowledge is essential in the study of the magnetic properties from a fundamental point of view. This is certainly a complicated subject, which gets even worse in amorphous systems where the lack of translational symmetry reduces drastically our possibilities of finding the atomic arrangements.

In order to get a more profound insight of the correlation between the structure and the magnetic properties in amorphous materials, it is convenient to chose simple systems like Fe-P or Co-P in which the reduced number of constituent simplifies the analysis of the experimental data concerning the structure. Both systems have been extensively studied from the point of view of their magnetic properties. Among others, Dietz and co-workers have investigated a series of Fe-P and Co-P samples in a wide range of compositions.[4,5] For these systems, in the amorphous region ($x>0.13-0.15$), the spontaneous magnetization decrease linearly with increasing P content, with the same slope for both systems. In contrast, the evolution of the Curie temperature T_c with composition is completely different. In the Fe-P alloys, it remains constant or changes very little with increasing P content (it seems to depend on the preparation method: in melt-quenched samples, T_c increases very slightly,[6–8] whereas in the electrodeposited ones, a decrease[9] or an insensitive[10] behavior has been reported). On the contrary, in Co-P alloys a steep decrease of T_c is observed.[4,8,11]

The fundamental magnetic properties such as the spontaneous magnetization and Curie temperature are mainly determined by the local environment of the metal atoms. In the Fe-P system, the Mössbauer spectroscopy has been extensively used to investigate this point.[9,12,13] There are also several studies of the structure using x-ray diffraction methods that allow us to extract the atomic radial distribution function.[14,15] In a previous work[13] we successfully used the EXAFS (extended x-ray absorption fine structure) spectroscopy to determine the evolution of the local structure of amorphous Fe-P alloys as a function of composition. This technique is an atom-selective local probe that permits us to obtain the coordination numbers and bonding distances, a very useful information in disorder systems since it is usually the only structural information that can be obtained.

The atomic structure of some Co-P amorphous alloys have been investigated by neutron diffraction by Sadoc *et al.*[16] and by Lagarde *et al.*[17] using the EXAFS technique. However, a thorough study in a wide range of compositions is still lacking.

In this paper we present a structural study by means of EXAFS of a complete series of amorphous Co-P alloys. We have also performed magnetic measurements in the very same set of samples. This allow us to correlate precisely the structure with the magnetic properties and its dependence on composition. This information is then used to study the implications of the different atomic structure of Fe-P and Co-P amorphous alloys on their different magnetic behavior. This comparison allow us to reveal what are the fundamental structural features that influence the magnetism in these alloys.

II. EXPERIMENT

A series of samples was prepared by electrodeposition from aqueous solutions following the procedure described elsewhere,[18] with compositions ranging from 15 to 26 at. % P. The samples were deposited onto copper substrates that were removed chemically after deposition. The resulting sample thickness was about 20 μm. To avoid possible inhomogeneities occurring during preparation due to edge effects, only the central part of the deposit was used for the

TABLE I. Spontaneous magnetization, magnetic moment per Co atom and Curie temperature for $Co_{1-x}P_x$ samples.

x	σ_0 (A m^2/kg)	μ_{Co} (μ_B)	T_c(K)
0.15	103	1.19	
0.17	92	1.07	644
0.18	84	0.99	625
0.20	75	0.90	557
0.22	66	0.80	452
0.26	52	0.65	301

experiments. The composition of the samples was estimated within 1 at. % P by emission plasma spectroscopy and x-ray energy-dispersive analysis. The samples were checked to be in a fully amorphous state by x-ray diffraction. This result is further confirmed by the lack of high-R structure of the EXAFS spectra.

Measurements of the saturation specific magnetization σ_s as a function of temperature were performed in a superconducting quantum interference device (SQUID) magnetometer from 5 to 400 K, and in a Faraday magnetometer above room temperature. In both cases a constant field of 1200 kA m^{-1} was used.

EXAFS experiments were performed at the Daresbury Laboratory Synchrotron facility running typically at 2 GeV and with an average current of 150 mA. The phosphorus K edge was measured in station 3.4 in total electron yield geometry using a double-crystal monochromator of InSb. The cobalt K edge was measured in station 7.1 in transmission geometry with a double-crystal Si(111) monochromator. All spectra were recorded at room temperature. Harmonic rejection, only necessary in the Co edge, was achieved by detuning the monochromator to reduce the intensity by 50%. The presence of a spurious jump corresponding to the sulphur K edge in the phosphorus absorption data reduces the EXAFS range available for the analysis. This, together with other experimental problems, made us discard the measurements of the P edge for all the samples but for the one with $x=0.22$, whose spectra is good enough to obtain reliable results.

III. DATA ANALYSIS AND RESULTS

A. Magnetization data

The saturation magnetization versus temperature $\sigma_s(T)$ curves yield a great amount of magnetic information. From the low temperature part of the curve, we obtained the values of the spontaneous magnetization at 0 K, σ_0, by extrapolating the fit of the low-temperature points to a $\sigma_s - T^{3/2}$ law, which results to be the best description of the data [see Fig. 4(a) below]. The implications of this kind of fit will be discussed in next section. The values of σ_0 so obtained, and their corresponding magnetic moment per Co atom, μ_{Co} (expressed in units of Bohr magnetons μ_B), are compiled in Table I. They show a linear decrease with increasing P content, and completely agree with those presented by Hüller *et al.*[4] in a very exhaustive study performed over a wide range of compositions, though they are significantly smaller than the ones reported before by other authors.[8,19] The extrapolation to $x=0$ gives a value very close to that of pure hcp Co ($\mu_{Co}=1.72\mu_B$).[20]

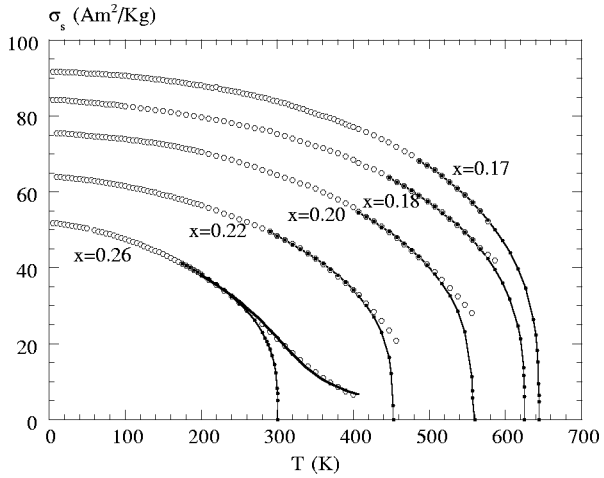

FIG. 1. Measured $\sigma_s(T)$ curves for $Co_{1-x}P_x$ samples (open circles). Full circles joined by the line, are the extrapolation to find T_c (see text). The line in sample $x=0.26$ is a fit to Eq. (1).

To achieve the complete saturation of the samples, the measurement of $\sigma_s(T)$ was performed at a relative high magnetic field. This, together with the fact that the crystallization temperature of the samples is close 600 K, make a involved task the analysis of high temperature data to obtain the Curie temperature. As can be observed in Fig. 1, the curves corresponding to samples with high P content reveal clearly the effect of the field by the presence of long tails in the $\sigma_s(T)$ curves. In the samples with lower P content, the onset of crystallization drastically reduces the available range for evaluation of T_c. In these circumstances we have opted to fit the high-temperature data to a critical law of the form $\sigma_s \propto (T-T_c)^{\beta}$. The same range of experimental points have been used in the fit for all the samples: only points corresponding to values of reduced magnetization σ_s/σ_0 greater that 0.75 are used. To give consistency to the process it is necessary to use similar values of the critical exponent β for all of the samples. Best fits are obtained using $\beta=0.32$ for samples with $x=0.26$ and $x=0.22$ and $\beta=0.31$ for the rest. The resulting extrapolations of the experimental points towards the value of T_c obtained from the fits are displayed in Fig. 1. This procedure allows to obtain a reasonable estimation of the Curie temperature whose values are compiled in Table I. However, since the effect of the high-magnetic field used in the measurement cannot be ignored, mostly in samples with the higher P content, we have also tried a fit to the equation of state that includes the field:[21]

$$\left(\frac{H}{M}\right)^{1/\gamma} = \frac{T-T_c}{T_1} + \left(\frac{M}{M_1}\right)^{1/\beta}, \qquad (1)$$

where T_1 and M_1 are parameters to be adjusted to fit the data. The fit for sample $x=0.26$ obtained with values of $\beta=0.32$ and $\gamma=4/3$ is also displayed in Fig. 1. The values of T_c obtained by this procedure are 10 to 50 degrees smaller (depending on the sample) than those yielded by the first method described. Neither of them are completely reliable. The fit to a critical law must be valid only in the very prox-

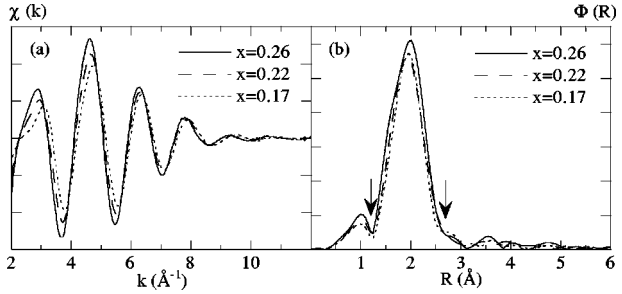

FIG. 2. (a) EXAFS signal $\chi(k)$ for some $Co_{1-x}P_x$ samples. (b) Fourier Transforms $\Phi(R)$ of the EXAFS functions. The arrows mark the width of the main peak used in the back Fourier transform.

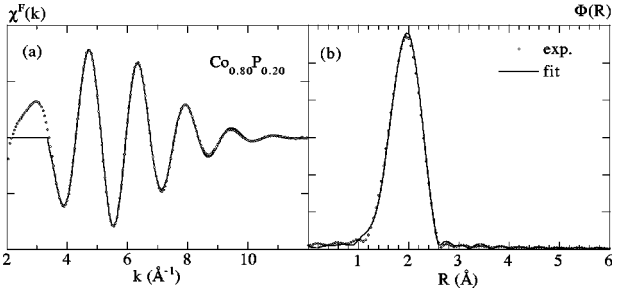

FIG. 3. Fourier filtered EXAFS function and fit in (a) *k* space and (b) *R* space.

imity of the Curie temperature. On the other hand, the equation of state of Eq. (1) is a first-order relation that must be not valid for large fields. In any case, the systematic variation of T_c over the range of compositions studied has the same trend in both cases. The values presented in Table I (obtained with the first procedure described) exhibit a linear decrease with increasing phosphorus content. The extrapolation to $x=0$ yields a value very close to the pure hcp Co ($T_c=1388$ K).[20] On the other end, the linear extrapolation gives $T_c=0$ for $x=0.33$. This result agrees rather well with the situation for the crystalline compound Co_2P that, with a small magnetization of $\sigma_s=5$ A m^2/kg (Ref. 11) is close to that limit. Other authors[4,8] report values of T_c that do not coincide exactly with ours. This is probably due to the difficulties described above and because of the alternative approaches used by these authors to determine T_c.

B. EXAFS data

1. Data analysis

From the experimental absorption curves, the normalized EXAFS functions $\chi(k)$ were obtained using the standard procedure.[22] Absorption above the edge was fitted using a three cubic-spline in the *k* range $2 \leqslant k \leqslant 12$ Å^{-1} for the Co *K* edge and a two-cubic spline in the range $2 \leqslant k \leqslant 9$ Å^{-1} for the P *K* edge. (This reduced range in the P is a consequence of the sulphur jump mentioned before). In all the spectra, the origin of *k* space was taken at the inflection point of the absorption edge.

The EXAFS signals obtained in this way for the Co *K* edge are displayed in Fig. 2(a). The $\chi(k)$ curves differ mainly at low *k* values, which is to be expected due to the greater scattering amplitude of P atoms in the range $3 \leqslant k \leqslant 5$ Å^{-1}. It is also possible to observe at first glance a small change in the frequency of oscillations, which is related with the changes in Co-Co bonding distances as will be discussed latter.

The Fourier transform of $\chi(k)$ is performed with a k^3 weight and a Hanning window function in the $2 \leqslant k \leqslant 12$ Å^{-1} range for the Co edge and in the $2 \leqslant k \leqslant 8$ Å^{-1} range for the P edge. These Fourier transforms present the characteristic single peak of amorphous alloys as shown in Fig. 2(b) for the Co edge. An inverse Fourier transform is then performed in the main peak (the selected range is marked with arrows in the figure). The resulting filtered EXAFS function $\chi^F(k)$ is finally compared with a model function using a least-squares fitting. The same range is used for all the samples: $3.5 \leqslant k \leqslant 11.5$ Å^{-1}. The quality of the obtained fits can be observed in Fig. 3, both in *R* and *k* space for sample $Co_{0.80}P_{0.20}$.

The extraction of structural data from EXAFS experiments relies on a structural model that is used to perform the fit. In the analysis of amorphous samples, a general approach in terms of the partial radial distribution function $g_j(r)$ (RDF) should be used. It has been confirmed that the use of Gaussian radial distribution functions in the analysis of EXAFS data from highly disordered systems gives rise to smaller interatomic distances than the real ones obtained by x-ray measurements. This difference is attributed to the occurrence of a very asymmetrical nearest-neighbor distribution.[23–25] For these materials, in the framework of a dense random packing of hard spheres model,[26] Crescenzi *et al.*[27] have proposed a RDF given by

$$g_j(r)=\begin{cases} \dfrac{1}{\sigma_{D_j}} e^{-(r-R_j)/\sigma_{D_j}} & \text{for} \quad r \geqslant R_j \\ 0 & \text{for} \quad r < R_j, \end{cases} \tag{2}$$

where R_j is the distance between the centers of the two touching spheres and σ_{D_j} is the root-mean-square displacement that gives the amount of structural disorder around its atomic site. The average distance is then given by $\overline{R_j}=R_j+\sigma_{D_j}$ as can be obtained by direct calculation on the RDF.

The EXAFS function can then be expressed as[28]

$$k\chi(k)=\sum_j \frac{N_j f_j(k,\pi)}{R_j^2} \frac{e^{-2\sigma_j^2 k^2} e^{-2\Gamma_j/k}}{\sqrt{1+4k^2\sigma_{D_j}^2}} \times \sin[2kR_j+\tan^{-1}(2k\sigma_{D_j})+\phi_j]. \tag{3}$$

Here, $f_j(k,\pi)$ is the backscattering amplitude function of atoms of type *j* around the absorbing species, *k* is the photoelectron wave vector, ϕ_j is the total phase shift, $\exp(-2\Gamma_j/k)$ is a mean-free path term that takes into account the inelastic losses, $\exp(-2\sigma_j^2k^2)$ is the Debye-Waller factor, and N_j is the number of atoms of *j* type around the absorbing one.

This expression has already been used to analyze the structure of different binary amorphous systems yielding good results in accordance with x-ray diffraction.[17,27,29] It has also been successfully used to analyze more complicated amorphous systems.[30]

TABLE II. Structural parameters obtained by EXAFS in $Co_{1-x}P_x$ samples. Errors are indicated between brackets. 10.0(9) means 10.0 ± 0.9.

x	N_{CoCo}	R_{CoCo} (Å)	$\sigma_{D_{CoCo}}$ (Å)	$\overline{R}_{CoCo}$ (Å)	N_{CoP}	R_{CoP} (Å)	$\sigma_{D_{CoP}}$ (Å)	$\overline{R}_{CoP}$ (Å)
0.17	10.0(9)	2.387(8)	0.16(1)	2.54(2)	2.0(7)	2.08(3)	0.25(9)	2.3(1)
0.18	10.0(6)	2.390(5)	0.16(1)	2.55(2)	2.2(3)	2.10(1)	0.20(9)	2.2(1)
0.20	10.1(7)	2.390(6)	0.15(1)	2.54(2)	2.2(4)	2.09(2)	0.24(5)	2.33(7)
0.22	9.8(7)	2.410(6)	0.15(1)	2.56(2)	2.5(4)	2.10(1)	0.22(4)	2.31(5)
0.26	9.0(9)	2.430(9)	0.13(2)	2.56(3)	2.7(6)	2.10(2)	0.18(5)	2.28(7)

To analyze the EXAFS data for our samples, we constructed model functions according with Eq. (3), where we used two shells corresponding to Co-Co and Co-P pairs for the Co K edge. For the P K edge we consider only P-Co pairs assuming that no P-P bondings exists.[31–33] Theoretical amplitudes and phase shifts were taken from FEFF6 codes.[34] We must note that in amorphous systems we cannot calculate them from a well-defined structural model using a cluster of atoms at fixed positions (as it is usually the input in FEFF for crystalline materials). We use instead the backscattering amplitudes and phase shifts calculated with only one atom of the adequate type (cobalt or phosphorous) acting as dispersor. The validity of these calculations is checked by fitting reference compounds: fcc Co, Fe_2P, $CoSi_2$, Fe_3Si, and Fe_2B. For those standards we fit the shells that contribute to the first peak in the Fourier transform. The results obtained were published in a previous work.[30] We assumed that these calculations, which are valid for Co-Si, Fe-Si, and Fe-P shells will also work with Co-P. We also use the fitting of the standards to extract the values of other parameters that take part in the EXAFS equation. In particular, Γ, related to the mean-free path of the photoelectron, is translated from Fe_2B, which is the standard whose structure is more similar to that of an amorphous system (lower symmetry and five shells of neighbors very close to each other in the range of 2–3 Å). Gamma is taken as $\Gamma = 1$ Å^{-1}, and kept the same for the fitting of all the amorphous samples. The origin of the threshold energy E_0 is also a parameter to be fitted for each shell. From the fitting of standards we learn that there is a constant difference of 2 eV between the values of E_0 for the metal (Co-Co or Fe-Fe) and metalloid (Fe-P, Fe-B, Fe-Si, or Co-Si) shells. We translate this result to our samples and let E_0 to be adjusted with this constrain. The value of S_0^2, which does not appear explicitly in Eq. (3), is already introduced in the amplitude calculation. We obtain a value for S_0^2 by fitting the standard compounds and recalculate the amplitudes for the fitting of the problem samples introducing this value in the FEFF input. Finally, we have used the same value of the Debye-Waller factor σ for all the samples ($\sigma^2 = 0.009$ Å^2). We therefore have six structural parameters left to be fitted (R, σ_D, and N for each shell). They are an excessive number considering that the number of independent data points is about 7 ($N_{ind} \approx 2\Delta k \Delta R/\pi$, where $\Delta k = k_{max} - k_{min}$ is the k-space fitting range and $\Delta R = R_{max} - R_{min}$ is the width of the R-space filter window[35]). In fact, if all six parameters are left free in the fitting, best fit results acquire unphysical values for some of the samples. Therefore, we first gave reasonable values to the coordination numbers, taking into account sample compositions, and fitted closest distances R and structural disorder σ_D. We then used the obtained closest distances R and fitted the coordination numbers and σ_D. The obtained values are those displayed in Table II. To check the validity of the results we have also performed other combinations, as fitting N, R, and σ_D for each shell (fixing the values for the other one), always obtaining values that are within the errors quoted.

2. Uncertainty analysis

The fitting procedure consists in the minimization of the difference between the Fourier filtered experimental data $\chi^F(k)$ and the model function $\chi(k)$ given by Eq. (3). The function to minimize is defined as

$$S^2 = \frac{\sum_{i=1}^{N} [\chi^F(k_i) - \chi(k_i)]^2 k_i}{\sum_{i=1}^{N} [\chi^F(k_i)]^2 k_i}. \tag{4}$$

This definition differs from the usual chi-square function, but avoids the normalization problems that affect the size of the calculated errors, which arise when uncertainties in experimental data are not well determined. The numerical minimization is performed using Minuit subroutine from the CERN program library.[36] Values of S^2 at best fit values are of the order of 2×10^{-5}. The uncertainty in the value of a variable is taken as the amount by which it can be increased until the value of S^2 reach a given limit. Following the recommendations of The International Workshop on Standards and Criteria in x-ray Absorption Spectroscopy,[35] this value was defined as double the value of S^2 at minimum. The fitting routine then gives the obtained uncertainties in the best parameters by inverting the matrix of second derivatives of S^2 with respect to the variable parameters.[36,37] As explained above, we could not fit all the structural parameters together. In order to present errors calculated in the same way for all the variables, the uncertainty displayed in Table II for each parameter was obtained by keeping all the others fixed. This procedure does not account for the influence of correlation between parameters, but we have checked that the errors obtained when more than one parameter are left free are the same order of magnitude. This is specially important for highly correlated variables such as coordination number and structural disorder. The magnitude of the errors is typical of EXAFS analysis: 10% in coordination numbers and below 0.1 Å in interatomic distances (0.03 Å for Co-P shell). It is to be noted that, in the case of the special function that we use for amorphous materials, the inter-

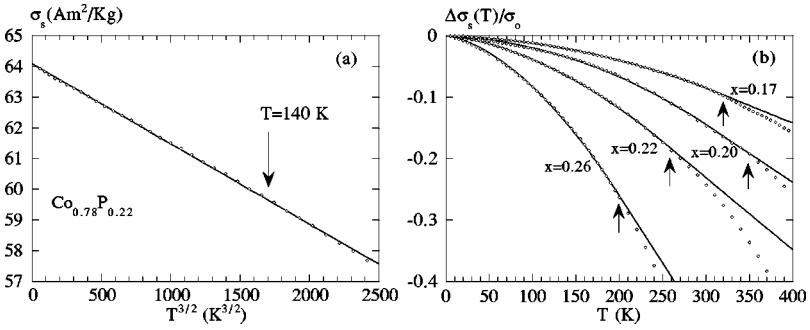

FIG. 4. (a) Spontaneous magnetization vs $T^{3/2}$ and linear fit. (b) Fit to Eq. (5). The arrows show the end of the fitting range.

atomic distance $\overline{R}$ is separated into two parameters: closest distances R and structural disorder σ_D. The first one is determined with considerable precision, as it is the main factor affecting the frequency of the oscillations. The structural disorder affects mainly the amplitude of the EXAFS signal and is highly coupled with the coordination number, and therefore affected by greater error. The quoted uncertainties in $\overline{R}=R+\sigma_D$ are obviously the sum of the ones for R and σ_D.

3. Results

The values of the best-fit parameters are presented in Table II. We must stress that we can have confidence in the results that we have obtained from the EXAFS analysis, because they correspond to a set of samples and we have followed the structural changes occurring systematically when changing the composition. No reliability can be assured if only one sample is fitted because of the number of parameters involved and the loose structural data that describes the structure. But, most important, data from only one sample is meaningless. Only the evolution of the structure with composition gives relevant information that can be correlated with changes in the magnetic behavior.

Previous structural results obtained by neutron diffraction in a sample of composition $Co_{0.81}P_{0.19}$ show a very good agreement with ours.[16] They found average distances of $\overline{R}_{CoCo}=2.54$ Å, and $\overline{R}_{CoP}=2.32$ Å. However, results obtained by EXAFS, using also an asymmetrical distribution function do not coincide so well with ours.[17] They report closest distances of $R_{CoCo}=2.43$ Å, $R_{CoP}=2.19$ Å, and average ones of $\overline{R}_{CoCo}=2.47$ Å, $\overline{R}_{CoP}=2.29$ Å in a sample that the authors claim to be of approximate composition $Co_{0.80}P_{0.20}$. The origin of the discrepancies could be precisely the uncertainty in the determination of sample composition. In both references, the coordination numbers are $N_{CoCo}=10$ and $N_{CoP}=1.5$ approx.

In our results, we focus on the evolution of the structural parameters in the whole range of compositions studied, and obtain a clear increase of the closest distances in the Co-Co bonding, R_{CoCo}, when the phosphorus content increases. The associated structural disorder, $\sigma_{D_{CoCo}}$ decreases, resulting in a slightly increasing (within the error bar) average distance $\overline{R}_{CoCo}$. The distances of the Co-P pairs remains unchanged, indicating the strong covalent nature of the bonding.

The values obtained for the coordination numbers are affected by greater errors, but a general trend can be observed, following the stoichiometric relation of the samples: N_{CoCo} decreases and N_{CoP} increases when the phosphorus content increases. Although these values are inside the error range, the increase of P atoms around the Co ones is reliable, as discussed before in the basis of the evolution of the amplitude of the raw EXAFS signal at low k values. We have observed that there is a strong correlation between coordination and the disorder parameter σ_D as both of them determine the amplitude of the EXAFS signal. We reiterate that our discussion rests in the systematic evolution of the parameters. Coordination numbers are to be driven by the stoichiometry of the samples, so the structural disorder evolution with composition must be real.

Due to the problems cited before, the analysis of the P edge could only be performed in sample $Co_{0.78}P_{0.22}$. The results [$N_{PCo}=8(2)$, $R_{PCo}=2.08(2)$ Å, $\sigma_{D_{PCo}}=0.23(5)$ Å, and $\overline{R}_{PCo}=2.31(7)$ Å] are coherent with the ones for the Co edge ($R_{PCo}=R_{CoP}$), confirming the validity of the results.

IV. DISCUSSION

Our aim is to discuss the results described before, mainly in comparison with the ones observed for the Fe-P system, which where reported in a previous work.[13] These systems present significant differences in the magnetic behavior, that we would like to correlate, whenever possible, with the differences found in the atomic structure.

Let us begin by analyzing the behavior of the spontaneous magnetization at low temperature. As can be seen in Fig. 4(a), for the Co-P system, the saturation magnetization $\sigma_s(T)$ at low temperature scales with a $T^{3/2}$ law. This result indicates that the decrease of the magnetization with the temperature is produced by the excitation of spin waves. Experiences of inelastic neutron scattering in a sample of $Co_{0.80}P_{0.20}$ (Ref. 38) confirm this fact by the observation of excitations that satisfy the usual dispersion relation of ferromagnetic materials: $\hbar\omega(k)=Dk^2$, where D is the stiffness constant and k is the spin-wave propagating vector. Following the Heisenberg model, the behavior of the saturation magnetization can then be expressed by

$$\frac{\Delta\sigma_s(T)}{\sigma_0}=\frac{\sigma_0-\sigma_s(T)}{\sigma_0}=BT^{3/2}+CT^{5/2}+\cdots. \qquad (5)$$

Our experimental data follow this relation in a wide range of temperature, up to $0.6T_c$, [much larger than in the case of crystalline Fe or Ni (Ref. 39)] as shown in Fig. 4(b). This behavior is also reported in more complex amorphous alloys like $Fe_{40}Ni_{40}P_{14}B_6$.[40] In the case of Fe-P amorphous alloys, the low-temperature saturation magnetization follows a T^2

law, up to very high values of temperature (close to $0.8T_c$).[13] This dependence can be attributed to a weak character of the ferromagnetism in the Fe-P system, in contrast with the $T^{3/2}$ dependence shown by Co-P, that is typical of a strong nature of the ferromagnetism.[41,42]

The specific magnetization at 0 K, σ_0, decreases linearly with increasing P content (Table I). This is the same behavior found for the FeP system in the range of compositions where the samples are completely amorphous. For samples with $x \lesssim 0.13$, there is a change in the slope for the Fe-P samples, which is related with the change in the number of neighbors from around twelve in the amorphous phase to eight in the bcc crystalline phase. The specific magnetization corresponding to a pure Fe sample, obtained by extrapolation from the measured values in the amorphous region gives a value much greater than $\sigma_0 = 222$ A m^2/kg, which is the value for bcc Fe. In the Co-P system, though a transition from amorphous to crystalline exits at about the same phosphorus concentration, the number of nearest neighbors remains about twelve and the $\sigma_0 - x$ line does not show any change in slope.

The origin of the reduction of the value of σ_0 with the increase of P content in the sample is often explained by the increasing electronic transference from the metalloid $3p$ band to the metal $3d$ band. This argumentation is controversial, most of all since no clear evidence of such transference has been found in photoemision experiments.[43] However, the increasing number of phosphorus atoms around the Co ones, and the evidence found in Fe-P amorphous alloys through the evolution of the isomer shift obtained by Mössbauer spectroscopy,[13] indicate that a certain degree of charge transfer can take place. In the framework of a rigid band model, and assuming a strong character of the ferromagnetism (that is, that the spin-up $3d$ subband is completely full), the magnetic moment per Co atom, μ_{Co} (in μ_B) is expressed as a function of the number of electrons transferred from each P atom, Z_P, as[44]

$$\mu_{Co} = \mu_{Co}^0 - \frac{x}{1-x} Z_P, \tag{6}$$

where μ_{Co}^0 is the magnetic moment in a pure cobalt sample. Using the data from Table I, a linear fit yields a value of $Z_P \simeq 3$. (The value obtained for μ_{Co}^0 is $1.7\mu_B$, in agreement with the corresponding for hcp Co).

The same approach, with the assumption of strong ferromagnetism, can be used for the Fe-P system. Using the data from Ref. 13, we obtain $Z_P \simeq 2$ (and $\mu_{Fe}^0 = 2.6\mu_B$, much greater than $2.22\mu_B$ that corresponds to bcc Fe, as discussed before). This result for Z_P is sensibly less than that obtained for the Co-P system. Assuming the P atoms donate the same number of electrons in both cases, the most simple explanation is that, while the Co-P system exhibits certainly a strong ferromagnetism, the Fe-P behaves as a weak ferromagnet system and, therefore, the electronic transference takes place to both spin-up and spin-down subbands. Thus, not every electron given by the phosphorus effectively reduces the iron magnetic moment.

The evidence brought about by the analysis of the magnetization data seems to state that both systems present different ferromagnetism character, strong for Co-P and weak for Fe-P. Very recent results obtained by x-ray magnetic circular dichroism performed on the metal K edge of Fe-P samples, confirms that the character of the ferromagnetism is weak for samples with low P content. However, the subject is still far from being clear, as a transition from weak to strong ferromagnetism has been detected at about 19% at. P.[45]

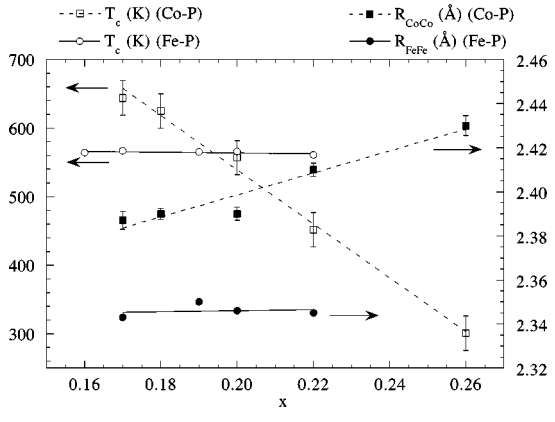

FIG. 5. Curie temperature, T_c, and closest metal-metal distances, R_{CoCo} and R_{FeFe}, for $Co_{1-x}P_x$ and $Fe_{1-x}P_x$ samples. The lines are linear fittings but serve as a guide to the eye. Error bars in T_c are orientative (see discussion in Sec. III A).

As stated before, considering the similarity of both systems, the more amazing result when comparing their behavior, is the completely different dependence of the Curie temperature on the P concentration. In the case of Fe-B amorphous alloys, that could be considered similar to Fe-P ones, the evolution of the T_c with increasing metalloid content shows a well defined increase,[46,47] in contrast with the constant value that presents the Fe-P system, but this distinct behavior is not so surprising because of the considerably different type of metalloid involved. For the case of Fe-P and Co-P we can try to correlate the different behavior with the structural results found by our EXAFS analysis. In the Fe-P system, neither the number of Fe neighbors N_{FeFe} nor the closest distances R_{FeFe} varies with composition, which is in clear contrast with the case of Co-P, where the number N_{CoCo} of neighbors increases with P (although not significantly), and the closest metal-metal distance R_{CoCo} suffers a considerable enhancement. This correlation can be observed in Fig. 5 where the Curie Temperature T_c and the closest distances, R_{FeFe} and R_{CoCo}, are represented as a function of composition. In this figure, the values are displayed using the same scale for both systems. While for Fe-P T_c and R_{FeFe} remain constant, for Co-P the decrease of T_c is accompanied by an increasing trend in R_{CoCo} distances.

In general, the Curie temperature is assumed to be proportional to the distance-dependent interatomic exchange integral $J(r)$ and to the coordination number of the magnetic species N_{MM} (M=Fe,Co). In the Fe-P alloys, the constant value of T_c could be then correlated with the lack of variation of both the distances and coordination numbers. In the Co-P system, the increasing interatomic distance would imply a reduction of the value of J, according with the shape of the Bethe-Slater curve.[48] The reduction of N_{CoCo}, though less significative, would also imply the decrease of T_c. These simple considerations also allow us to explain the be-

havior of T_c in the Fe-B system, where, according with very recent results, still to be published, the closest Fe-Fe distance increases with the B content which, in accordance with the Bethe-Slater curve, means an increase in the value of J.

Although our results seems to explain the differences in T_c on a structural basis, we must recall that we are dealing with amorphous alloys, whose atomic arrangement is described by a radial distribution function [given by Eq. (2) in our model]. In this case, the Curie temperature is more realistically described by[49]

$$T_c \propto \int J(r)g(r)d^3r, \tag{7}$$

which obviously depends not only on the closest distances, but also on the structural disorder σ_{MM}. It would therefore seem to be more reasonable to analyze the results using the mean interatomic distances $\overline{R}_{MM}=R_{MM}+\sigma_{MM}$ than the closest distances R_{MM}. However, as stated before, it is the value of the closest distance the one that can be determined with considerable precision. The parameter associated with the structural disorder is highly coupled with the coordination number in the fitting procedure and the obtained values are less reliable for the analysis we have performed.

In definitive, we have experimental evidence of the existence of a clear correlation between the structure and the magnetic behavior but it is difficult to go further than a qualitative interpretation of the consequences of that circumstance.

In any case, these differences in the dependence of T_c on composition are a consequence of the differences in the structure. It has been observed that there exists a preferred chemical affinity of phosphorus for the cobalt rather than for the iron when both types of metal are present, as it is the case in Fe-Co-P amorphous alloys.[50,51] Such chemical affinities have also been observed in Fe-Co-Si-B samples, where the preferred bondings are Fe-B and Co-Si.[30,50] It is to be expected that these distinct affinities affect the bonding characteristic of Fe-P and Co-P pairs, and therefore, the structure of the binary alloys Fe-P and Co-P.

V. CONCLUSIONS

The structure of a series of $Co_{1-x}P_x$ amorphous alloys, studied by EXAFS spectroscopy, has been shown to vary with the metalloid content x. The Co-Co interatomic distance increases, specially the closest one. The distance Co-P remains unchanged due to the covalent nature of the bond. The Co-Co coordination number seems to increase slightly while the Co-P increases following the stoichiometry of the samples.

The magnetic properties measured in the same samples confirms the previous results from other authors and show that the spontaneous magnetization at 0 K and the Curie temperature decrease linearly with x. The low-temperature magnetization follows a $T^{3/2}$ law.

These properties are in contrast with those presented by the Fe-P amorphous alloys. The different ferromagnetic character of both systems, strong for Co-P and weak for Fe-P, is suggested by the analysis of the magnetic properties, but can only be definitively stated by determination of the electronic structure. However, the differences in the dependence of the Curie temperature on composition can be qualitatively correlated with the structural differences through the variation of the exchange integral with the interatomic distance.

Even in very simple systems like the ones studied, composed by very similar atomic species, exist great differences in the magnetic behavior and their relation with the atomic structure are difficult to be established. Though very interesting correlations have been presented in this work, the problem is still not completely understood.

ACKNOWLEDGMENTS

This work has been supported by the Spanish CICyT under Project No. MAT96-1023. The authors thank the Daresbury Laboratory for the use of the synchrotron radiation facility, and Dr. J. A. Blanco and Dr. Alberto García for useful comments.

[1] *Amorphous Metalic Alloys*, edited by F. E. Luborsky (Butterworths, London, 1983).
[2] *Metallic Glasses: Magnetic, Chemical and Structural Properties*, edited by R. Hasegawa (CRC, Boca Raton, FL, 1983).
[3] K. Moorjani and J. M. D. Coey, *Magnetic Glasses* (Elsevier, Amsterdam, 1984).
[4] K. Hüller, G. Dietz, R. Hausmann, and K. Kölpin, J. Magn. Magn. Mater. **53**, 103 (1985).
[5] F. Stein and G. Dietz, J. Magn. Magn. Mater. **117**, 45 (1992).
[6] M. Takahashi and M. Koshimura, Jpn. J. Appl. Phys. **16**, 2269 (1977).
[7] M. Mitera, M. Naka, T. Masumoto, N. Kazama, and K. Watanabe, Phys. Status Solidi A **49**, K163 (1978).
[8] N. S. Kazama, T. Masumoto, and M. Mitera, J. Magn. Magn. Mater. **15-18**, 1331 (1980).
[9] J. Logan and E. Sun, J. Non-Cryst. Solids **20**, 285 (1976).
[10] K. Hüller and G. Dietz, J. Magn. Magn. Mater. **50**, 250 (1985).
[11] D. Pan and D. Turnbull, J. Appl. Phys. **45**, 1406 (1974).
[12] E. P. Elsukov, Yu. N. Vorobev, A. V. Trubachev, and V. A. Barinov, Phys. Status Solidi A **117**, 291 (1990).
[13] A. García-Arribas, M. L. Fdez-Gubieda, I. Orue, and J. M. Barandiarán, Phys. Rev. B **44**, 4146 (1991).
[14] J. Logan, Phys. Status Solidi A **32**, 361 (1975).
[15] E. J. Hiltunen, J. A. Letho, and L. Takacs, Phys. Scr. **34**, 239 (1986).
[16] J. F. Sadoc and J. Dixmier, Mater. Sci. Eng. **23**, 187 (1976).
[17] P. Lagarde, J. Rivory, and G. Vlaic, J. Non-Cryst. Solids **57**, 275 (1983).
[18] J. Herreros, J. M. Barandiaran, and A. García-Arribas, J. Non-Cryst. Solids **201**, 102 (1996).
[19] R. W. Cochrane and G. S. Cargill III, Phys. Rev. Lett. **32**, 476 (1974).
[20] Charles Kittel, *Introduction to Solid State Physics*, 7th ed. (Wiley, New York, 1996), p. 449.

[21] A. Arrott and J. E. Noakes, Phys. Rev. Lett. **19**, 786 (1967).
[22] B. Lengeler and P. Eisenberger, Phys. Rev. B **21**, 4507 (1980).
[23] E. D. Crozier, J. J. Rehr, and R. Ingalls, in *X-Ray Absorption: Principles, Applications and Techniques of EXAFS, SEXAFS, and XANES*, edited by D. C. Koningsberger and R. Prins (Wiley, New York, 1988), Chap. 9.
[24] P. Eisenberger and G. S. Brown, Solid State Commun. **29**, 481 (1979).
[25] R. Haensel, P. Rabe, G. Tolkiehn, and A. Werner, in *Liquid and Amorphous Metals*, edited by E. Lüscher and H. Coufal (Sijthoff and Nordhoff, Alphen aan den Rijn, The Netherlands, 1980), p. 232.
[26] J. L. Finney, Nature (London) **266**, 309 (1977).
[27] M. Crescenzi, A. Balsatori, F. Comin, L. Incoccia, S. Mobilio, and N. Motta, Solid State Commun. **37**, 921 (1981).
[28] For a more detailed deduction of Eq. (3), see, for example, Ref. 13.
[29] S. Mobilio and L. Incoccia, Nuovo Cimento **3**, 846 (1984).
[30] M. L. Fdez-Gubieda, I. Orue, F. Plazaola, and J. M. Barandiarán, Phys. Rev. B **53**, 620 (1996).
[31] J. D. Bernal, Nature (London) **185**, 68 (1960).
[32] D. E. Plok, Scr. Metall. **4**, 117 (1970).
[33] J. Wong and H. H. Liebermann, Phys. Rev. B **29**, 651 (1984).
[34] S. I. Zabinsky, J. J. Rehr, A. Ankudinov, R. C. Albers, and M. J. Eller, Phys. Rev. B **52**, 2995 (1995).
[35] F. W. Lytle, D. E. Sayers, and E. A. Stern, Physica B **158**, 701 (1989).
[36] F. James, *MINUIT Function Minimization and Error Analysis. Version 94.1 Reference Manual*, CERN Program Library entry D506 (CERN, 1994).
[37] P. R. Bevington, *Data Reduction and Error Analysis for the Physical Sciences* (McGraw-Hill, New York, 1966).
[38] H. A. Mook, N. Wakabayashi, and D. Pan, Phys. Rev. Lett. **34**, 1029 (1975).
[39] B. E. Argyle, S. H. Charap, and E. W. Pugh, Phys. Rev. **132**, 2051 (1963).
[40] S. N. Kaul, Phys. Rev. B **24**, 6550 (1981).
[41] B. Barbara, D. Gignoux, and C. Vettier, *Lectures on Modern Magnetism* (Springer-Verlag, Berlin, 1998), p. 149.
[42] F. Gautier, in *Magnetism of Metals and Alloys*, edited by M. Cyrot (North-Holland, Amsterdam, 1982), p. 13.
[43] J. Hafner, M. Tegze, and Ch. Becker, Phys. Rev. B **49**, 285 (1994).
[44] H. Yamauchi and T. Mizoguchi, J. Phys. Soc. Jpn. **39**, 541 (1975).
[45] M. L. Fdez-Gubieda, I. Orue, P. Gorria, A. García-Arrihas, J. M. Barandiarán, R. López, S. Pizzini, and A. Fontaine, J. Magn. Magn. Mater. **196-197**, 204 (1999).
[46] R. Hasegawa and R. Ray, J. Appl. Phys. **49**, 4174 (1978).
[47] C. L. Chien and K. M. Unruh, Phys. Rev. B **24**, 1556 (1981).
[48] For a schematic diagram of the Bethe-Slater curve see, for instance, B. D. Cullity, *Introduction to Magnetic Materials* (Addison Wesley, Reading, MA, 1972), p. 134.
[49] T. Kaneyoshi, *Amorphous Magnetism* (CRC Press, Boca Raton, FL, 1984), p. 33.
[50] M. L. Fdez-Gubieida, A. García-Arribas, I. Orue, F. Plazaola, and J. M. Barandiarán, Europhys. Lett. **40**, 43 (1997).
[51] A. García-Arribas, M. L. Fdez-Gubieda and J. M. Barandiarán, J. Magn. Magn. Mater. **196-197**, 164 (1999).